2024-05-01

Biofabrication Of Human Tissue-On-A-Chip Models Using Engineered Biocompatible Electrospun Scaffolds

Zayra Naomi Dorado
University of Texas at El Paso

BIOFABRICATION OF HUMAN TISSUE-ON-A-CHIP MODELS USING ENGINEERED BIOCOMPATIBLE ELECTROSPUN SCAFFOLDS

ZAYRA NAOMI DORADO

Master's Program in Metallurgy and Materials Science Engineering

APPROVED:

Binata Joddar, Ph.D., Chair

David A. Roberson, Ph.D.

Armando Varela-Ramirez, Ph.D.

Stephen L. Crites, Jr., Ph.D.
Dean of the Graduate School

Dedication

I dedicate this to my parents and siblings, who were there from the very first day of this journey. To my friends who have become family, for their constant support and never letting me doubt myself. Your continuous support, prayers, and guidance have gotten me through every accomplishment. God is good all the time.

I dedicate this to my dad. Papá: You were right, "It is what it is".

BIOFABRICATION OF HUMAN TISSUE-ON-A-CHIP MODELS USING ENGINEERED BIOCOMPATIBLE ELECTROSPUN SCAFFOLDS

by

ZAYRA NAOMI DORADO, B.S.

THESIS

Presented to the Faculty of the Graduate School of

The University of Texas at El Paso

in Partial Fulfillment

of the Requirements

for the Degree of

MASTER OF SCIENCE

Department of Metallurgical, Materials, and Biomedical Engineering

THE UNIVERSITY OF TEXAS AT EL PASO

May 2024

Acknowledgments

My sincere appreciation to my advisor and committee chair, Dr. Binata Joddar, for her imminent support through the completion of my graduate studies. I am grateful for the valuable exposure and opportunity to work at the Inspired Materials & Stem-Cell Based Tissue Engineering Laboratory (IMSTEL). To our collaborators, Dr. Yoshihiro Ito and Dr. Abosheasha from RIKEN, Japan, for allowing me to work with such novel materials. I would also like to thank Dr. David Roberson for the extensive material characterization lessons and for trusting me to operate several Polymer Extrusion Laboratory (PEL) Equipment. As well, I would like to thank Dr. Armando Varela for guiding me in completing this project, for the biology immersion and the shared concepts, and for serving on my defense committee. Additionally, I would like to thank Dr. Natividad-Diaz and the 3D Printed Microphysiological Systems Laboratory (3DPMS) lab members for their infinite help.

To the faculty and staff members who helped me along the way, Dr. Christopher Bradley, for his expertise in the MME field. Dr. Edgar A. Borrego Puerta, thank you for your extensive guidance, assistance, and patience during numerous training sessions in the BBRC.

I am grateful to the PASSE faculty and members for the funding opportunity to undertake my studies at the Department of Materials and Metallurgical Engineering, University of Texas at El Paso.

Finally, I would like to express my deepest gratitude to my support system and the people who provided me with encouragement and wisdom. To my family, who kept cheering on my back, to my colleagues who pushed me to challenge myself, to my classmates who made this journey enjoyable, and to the lifelong friends this degree has given me.

Abbreviations

Myocardial infarction (MI), furfuryl gelatin (F-gelatin/f-gel), poly-caprolactone (PCL), native tissue (NT), extracellular matrix (ECM), SEM (Scanning Electron Microscopy), Backscatter electron (BSE), ultra-variable detector (UVD), FTIR-ATR (Fourier-Transform Infrared – Attenuated Total Reflectance), and DMA (Dynamic mechanical analysis), optical microscopy (OM), direct current (DC), Liquid-crystal display (LCD), dynamic mechanical testing machine (DMA).

Abstract

This study explored the adoption of furfuryl gelatin (F-gelatin) based electrospun scaffolds compared with poly-caprolactone (PCL) as promising biomaterials for tissue engineering applications. Tissue-on-a-chip models, incorporating F-gelatin and PCL electrospun scaffolds, offer promising avenues for healthy and disease-in-vitro tissue models that can be explored to investigate underlying physiological mechanisms involved in disease development. Previous research has demonstrated the cytocompatibility of F-gelatin when used for modifying implant surfaces and tissue repair applications [1]. Our earlier published works have also successfully utilized F-gelatin for in-vitro cardiac tissue engineering [2][3]. We designed F-gelatin and PCL electrospun scaffolds to replicate the native tissue extracellular matrix (NT-ECM) environment. Additionally, we hypothesized that blending the hydrophilic F-gelatin with hydrophobic PCL would result in mechanically robust scaffolds capable of supporting the retention and viability of cells, essential for establishing a successful in-vitro tissue model. Since the electrospinning method offers versatility in controlling fiber alignment and composition, allowing for the generation of scaffolds that closely resemble the NT-ECM, we aim to optimize the electrospinning parameters to yield scaffolds that possess excellent mechanical fidelity, biocompatibility as well as the ability to sustain long-term culture periods. Specifically, we will study the effects of optimizing electrospinning parameters such as rotational speed, deposition distance, and voltage to evaluate their impact on the resultant scaffolds. Two collection speeds, static (0 RPM) and dynamic (>100 RPM), will be compared to assess their effects on scaffold fiber alignment as well as orientation and its correlation with the scaffold's biological properties.

To facilitate these experiments, we have developed an in-house electrospinning system capable of recording the various electrospinning parameters via an Arduino setup, which has led to reliable

and reproducible results for tissue engineering applications [4]. Samples will be characterized for mechanical fidelity via SEM (Scanning Electron Microscopy), FTIR-ATR (Fourier-Transform Infrared – Attenuated Total Reflectance), and DMA (Dynamic Mechanical Analysis). Finally, three different applications will be developed using these scaffolds, including their use in 1) seeding and differentiation of neural progenitor cells for studying neurodegenerative diseases, 2) for the development of cardiac cell models to study the onset of diabetes, and 3) adoption in tissue-on-a-chip models to be tested under microgravity and other extreme environmental conditions. Overall, this project contributes to developing novel NT-ECM for biocompatible human tissue-on-a-chip models via the biofabrication of electrospun scaffolds.

Table of Contents

List of Illustrations

List of Tables

List of Figures

Chapter 1: Introduction

BACKGROUND

Cardiac Tisue-on-a-chip Model

Myocardial infarction (MI) is one of the leading causes of morbidity and mortality worldwide, caused by the irreversible death of cardiomyocytes in the heart wall. The loss of these terminally differentiated cardiomyocytes during MI leads to a significant reduction in contractile efficiency, subsequently causing long-term heart failure. The need for more reliable human model systems for studying cardiac diseases has hindered our understanding of the cellular processes and molecular mechanisms during heart disease progression. Studies have attempted to model cardiac tissues through traditional tissue engineering approaches to understand heart diseases at their initial stages.

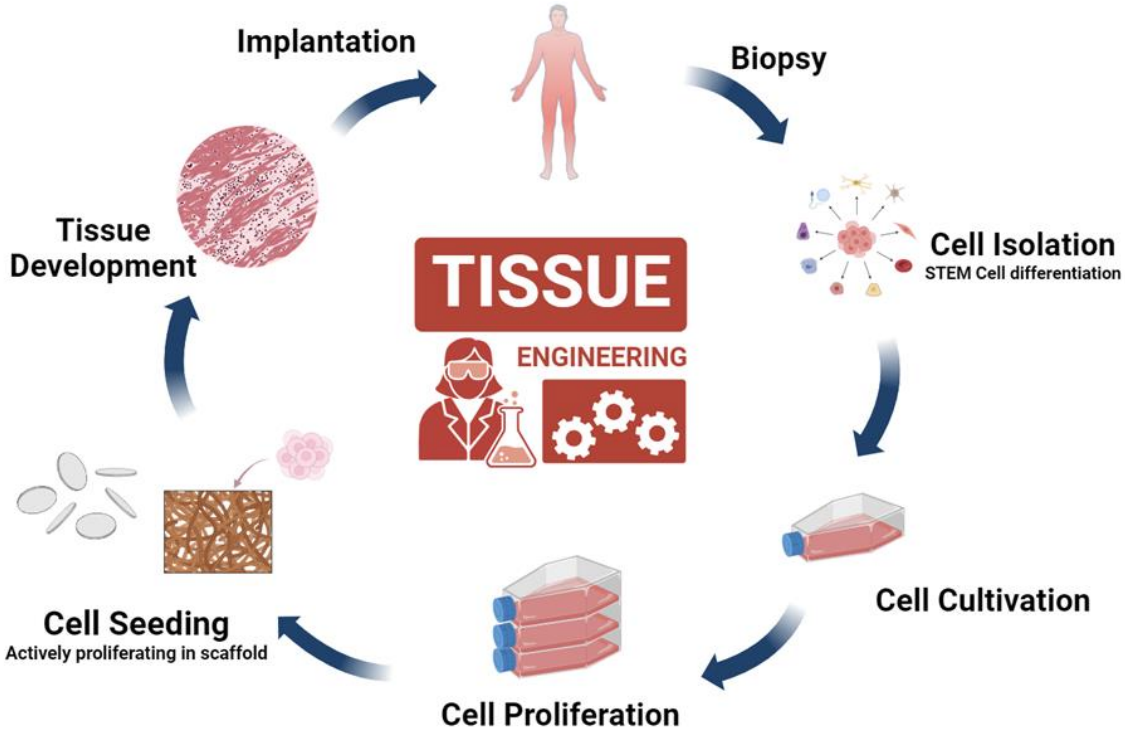

Illustration 1. Tissue Engineering diagram from biopsy to implantation steps. Created with BioRender.com.

One of the significant goals in tissue engineering involves the development of ideal scaffolds for regenerating damaged tissue and organs. Nanofibrous scaffolds are suitable for cell attachment and proliferation due to their similarity to the native tissue (NT) extracellular matrix (ECM). However, traditional scaffolds often possess inherently low mechanical and handling properties, posing a disadvantage. Addressing these challenges, researchers have turned to advanced tissue engineering techniques like electrospinning, which offers versatility in generating nanofibers from various materials, including polymers, composites, and ceramics.

Electrospun fibrous scaffolds, with their high surface area-to-volume ratios and superior mechanical properties, have been applied in diverse areas like wound healing, tissue engineering, and drug delivery. [6]. By providing a 3D construct for the seeding of cardiomyocytes, the array translates into a tissue-on-a-chip model where diverse cell culture applications can be studied further. Moreover, ECM-mimicking constructs laden with stem cells hold promise for in vivo transplantation as they reduce the probability of an immune response, given that the cells are obtained autologously from patients. Electrospun scaffolds are poised to revolutionize cardiac repair, potentially transforming treatment options and improving outcomes for patients with heart disease through advancements in ECM-mimicking constructs and stem cell technologies**.**

Electrospinning (ES)

Nanofibrous biomaterials emerge from four primary areas: biological applications, the physics of Taylor cone formation, material selection in electrospinning, and the influence of environmental conditions on the fabrication process. Nanofibers have garnered significant interest in biomedical engineering, particularly in nanoscience and nanotechnology. [7].

This technique benefits from applying a high electric field to produce ultra-fine polymeric fibers that range from micro- to nanometer diameters. The primary mechanism behind this technique is

a complex electro-physical activity between the polymer solution and the applied electrostatic force. Electrospinning generates a high-voltage electric field between the tip of the metallic needle and the collecting surface with a strong power supply and electrodes. When a high voltage is applied, the polymeric solution is gradually forced out from the syringe, causing a semirounded droplet to be shaped at the tip of the needle. This polymer droplet lengthens into a conical shape, known as the Taylor cone, and the surface charge on the polymer droplet increases with time by increasing the voltage [8]. A polymer jet starts to form immediately after overcoming the surface charge of the polymer droplet. After vaporizing the solvent in the polymer jet, the surface charge increases, destabilizing the polymer jet. The polymer jet is geometrically segregated, initially into two jets and, eventually, into many jets, to compensate for the instability. The electrostatic force, which affects the constantly splitting polymer droplets, causes the nanofiber patterning. Following Illustration 1Illustration 2, the standard electrospinning system's main constituents are a high-voltage power supply, a grounded collector, a syringe with a metallic needle, and a syringe pump [8]. The processing flexibility of electrospinning facilitates the production of various polymeric fibers for numerous applications.

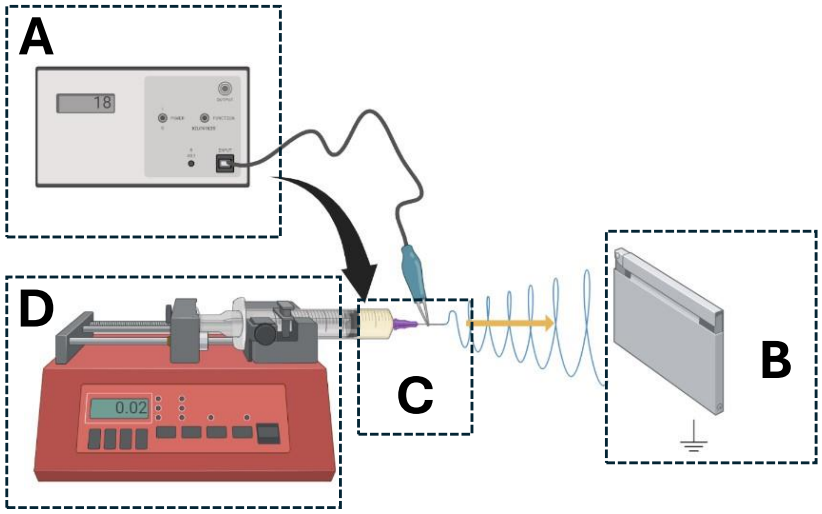

Illustration 2. Standard Electrospinning System Constituents. A) High-voltage power supply; B) Grounded Collector; C) Syringe with metallic needle; D) Syringe Pump. Created with BioRender.com.

GOALS

In this research, we aimed to create poly-caprolactone (PCL) and furfuryl-gelatin (F-gelatin) based electrospun scaffolds specifically for cardiac tissue modeling. PCL, which possesses higher degradation rates and cost-effectiveness, facilitates the creation of a workable structure that serves as an initial matrix component for cell-based scaffolding in tissue engineering.

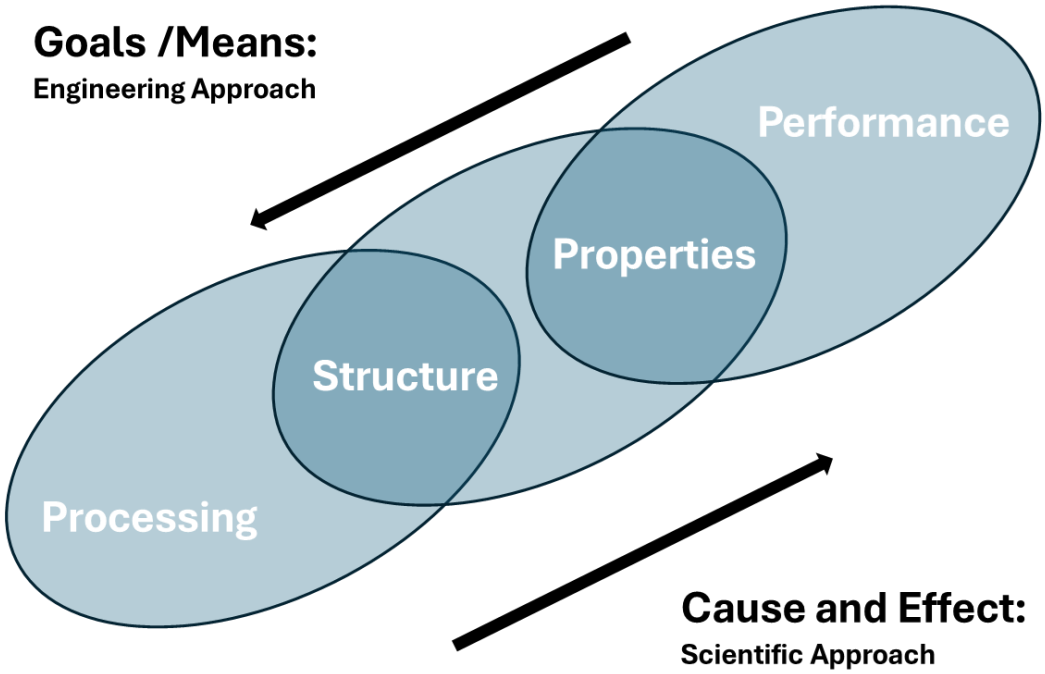

Figure 1. Representation of the Materials Paradigm

The workability of this polymer enables the rapid fabrication of novel scaffolding platforms as no further processing steps are required for the matrix to be stabilized and sustain mechanical fidelity, which further establishes PCL as a leading biomaterial for applications in regenerative medicine. Poly-caprolactone (PCL) is a hydrophobic biodegradable polymer widely employed to craft cardiac tissue scaffolds. While PCL boasts high mechanical stability, it lacks inherent reactive sites conducive to cell adhesion. On the other side, Gelatin, favored for its biodegradability, cost-

effectiveness, and the presence of cell-adhesive RGD (Arg-Gly-Asp) sequences, is also a top choice for biofabricating cell-based scaffolds in tissue engineering. Its minimal immunogenicity and the capacity for modification to improve both biochemical and mechanical characteristics. Traditional methods of crosslinking gelatin, using either enzymes or chemical agents like glutaraldehyde, often result in toxicity. Son et al. pioneered a technique to make gelatin crosslinkable with visible light by incorporating furfuryl groups to circumvent this. [4]. We previously applied this pioneering F-gelatin compound in our scaffold biofabrication, which enabled us to study the interactions between STO fibroblasts and C2C12 myoblasts. extensively [4].

TECHNOLOGY DEVELOPMENT

In this study, four types of electrospun scaffolds, PCL and F-gelatin, were developed through single nozzle electrospinning where the first set was collected in a static conductive plate, and the second set of samples was collected in a dynamic form by a rotating conductive roll. The physical, mechanical, and biological performance of these hybrid nanofibrous scaffolds as platforms for growing cardiac cells were evaluated in this study. The electrospinning parameters were optimized for all scaffolds, and their structural and mechanical integrity were characterized through optical microscopy (OM), scanning electron microscopy (SEM), and FTIR-ATR (Fourier-Transform Infrared – Attenuated Total Reflectance). Scanning electron microscopy revealed uniform fibrous structures with diverse orientations. The static collection showed curled fibers through the structure, while dynamic acquisition revealed fairly oriented fibers. The average F-gelatin scaffold depicted the formation of a ribbon-like fiber structure with varying diameters of 702 ±174 nm (F-gelatin) and 841±357nm (PCL), respectively. The average F-gelatin scaffold thickness is 90 µM, whereas the average PCL scaffold thickness is 20 µM.

Chapter 2: Materials

MATERIALS

Furfuryl–gelatin or F-gelatin was prepared by homogeneous addition of furfuryl glycidyl ether to a porcine gelatin solution and supplied by our collaborators Dr. Yoshihiro Ito and Dr. Abosheasha from RIKEN, Japan. Phosphate Buffered Saline (10X Solution) and 1,1,1,3,3,3 hexafluoroisopropanol (HFIP) were purchased from Fisher Bioreagents, USA. Polycaprolactone (PCL), of an average of Mn 80,000, was purchased from Sigma Aldrich (St Louis, MO, USA).

Polycaprolactone (PCL)

PCL is a synthetic polymer that is partially crystalline, which poses a low melting point of approximately (60°C) and a glass transition temperature of −60°C. It is made by ring-opening polymerization of ε-caprolactone. Lipases and Esterases of microorganisms can readily degrade PCL.[10]

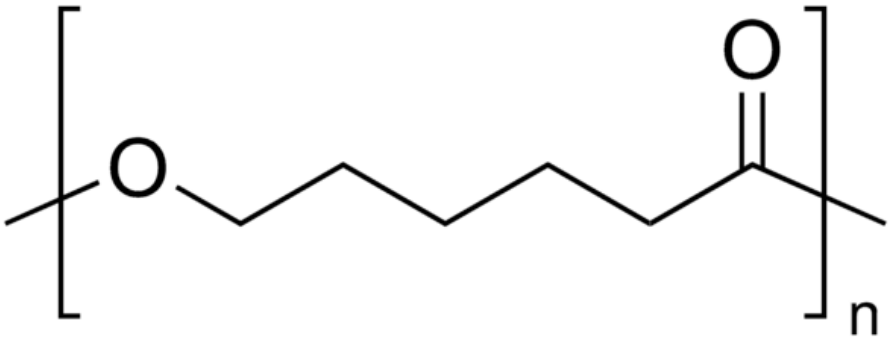

Figure 2. Poly(ε-caprolactone) molecule.

Due to its chemical and biological properties, as well as its physicochemical state, polycaprolactone (PCL) is notable for its adjustable degradability and mechanical strength. This allows it to maintain its properties under extreme mechanical, physical, and chemical conditions. PCL's degradation time is relatively long, which aligns well with its primary use as a replacement for hard tissues in the body, where healing also requires an extended period. Consequently, this material is ideal for use as a matrix in lengthy in vitro studies, where a 2D culture would be less

effective. Additionally, PCL's versatility extends to the engineering of soft tissues by modifying its molecular weight and degradation time, thus broadening its applicability across different types of tissue engineering. [12].

Furfuryl- Gelatin (F-gelatin)

F-gelatin is a natural polymer synthesized through the homogeneous combination of porcine gelatin powder and furfuryl glycidyl ether. The preparation process, according to protocols provided by our collaborators, involved the use of porcine gelatin powder and furfuryl glycidyl ether (96%), obtained from Sigma-Aldrich, along with DMSO sourced from Duchefa Biochemie (Haarlem, The Netherlands), and Sodium hydroxide (NaOH), hydrochloric acid (HCl), acetone, and ether procured from Duksan Pure Chemical Co., Ltd (South Korea).

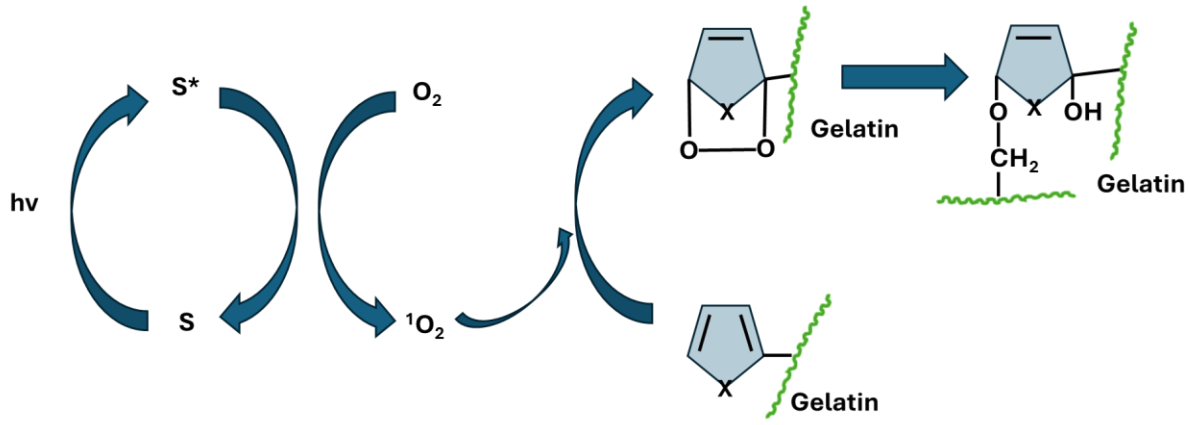

Figure 3. Inspired By T.I. Son et al. / Acta Biomaterialia 6 (2010) 4005–4010
Schematic drawing of the photo-oxidation crosslinking (POC) mechanism. F-gelatin formation.

To prepare F-gel, (2 g) of porcine gelatin was dissolved in (80 mL) of double-distilled water, and with a 1N NaOH solution, the pH was adjusted to 11. Subsequently, (250 µL) of furfuryl glycidyl ether was dissolved in (20 mL) of DMSO and added to the gelatin solution at room temperature. The mixture was then stirred for 30 hours at 65°C. After reaching a pH of 7 with 1N HCl solution, the resulting mixture underwent dialysis in deionized (DI) water for 48 hours using a dialysis membrane with a molecular weight cut-off of 1000 Da (Spectrum Laboratories Inc.,

Rancho Dominguez, CA). The dialyzed solution was then evaporated, and the purified F-gelatin underwent multiple washes with acetone followed by ether before being dried.

The dried F-gelatin was characterized using 1H nuclear magnetic resonance (NMR) spectroscopy with a Gemini 2000 spectrometer (300 MHz, Varian Inc., Palo Alto, CA). For analysis, both porcine gelatin (control) and F-gelatin were dissolved in deuterium oxide (D2O, Sigma), and the NMR spectra obtained were scrutinized to confirm the derivatization of gelatin into F-gelatin. [1][5][15]

Our lab has implemented furfuryl-gelatin as a novel, visible-light crosslinkable biomaterial for fabricating cell-laden structures with high viability. The use of F-gelatin has now been widely explored in different applications for fabrication in tissue engineering and biomedical engineering areas, such as biocompatible ink for 3D printing applications. [13]. Due to its superior cytocompatibility properties, rapid crosslinking mechanisms, and structural fidelity, we opted to continue exploring the applications of this material with the development of coating mechanisms to enhance cell viability and evaluate cell proliferation on 3D constructs for experimental setups of extended longevity. [14]

Chapter 3: Methods

System Prototyping and Optimization

Electrospinning Standard IMSTEL setup

The apparatus used for single fiber production was developed in-house following. Illustration 3. Scheme of IMSTEL electrospinning setup. Created with BioRender.com.. A grounded electrical mat was placed in a Laser Engraver-Pro enclosure (JIICCODA) to serve as a working platform. Subsequently, a syringe pump from New Era Pump Systems, Inc. was placed inside the chamber.

The high-voltage DC supply was procured from (ES30P 10 W power supply, Gamma High Voltage Research, Ormond Beach, FL) and was located on the outside left portion of the enclosure; connections were placed through lateral orifices of the chamber.

Exhaust ventilation was located on the right side of the enclosure, allowing the solvent fumes to be extracted safely.

Two sensors located in the inner central portion of the chamber recorded ambient temperature and humidity and displayed on a Liquid-crystal display (LCD) located on the outer right side of the enclosure.

Sensor placement was determined by tracing temperature and humidity levels at different points throughout the chamber with the help of an Arduino setup.

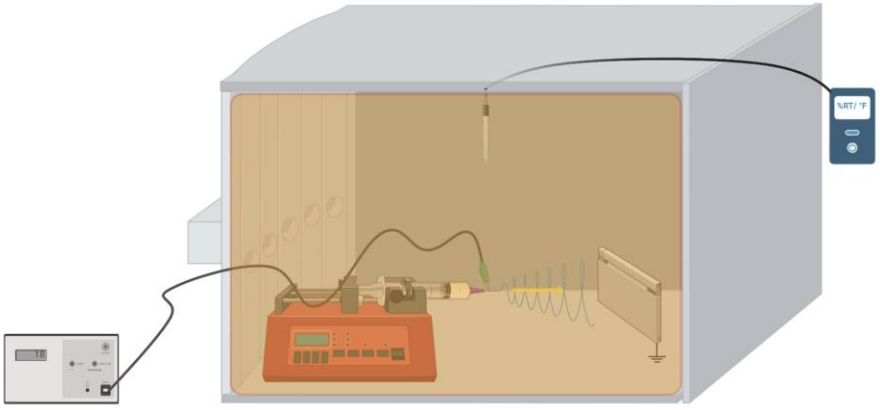

Illustration 3. Scheme of IMSTEL electrospinning setup. Created with BioRender.com.

Static vs Dynamic setup

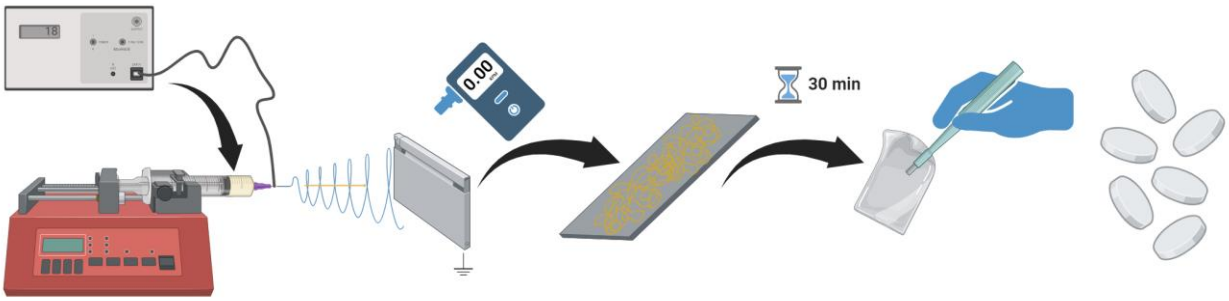

Illustration 4. Scheme of the development of random electrospun fibers, where the collector remains static. Created with BioRender.com.

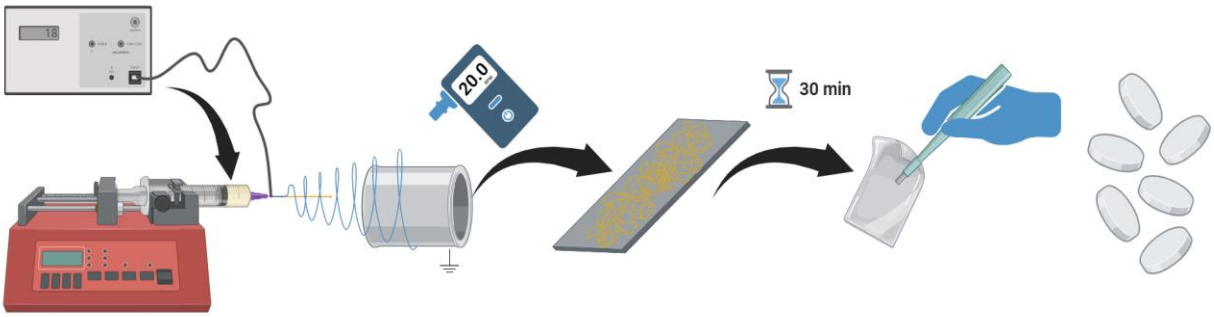

Illustration 5. Scheme of the development of semi-aligned electrospun fibers, where the collector is rotating. Created with BioRender.com.

A static collector was created by placing an aluminum substrate on a plastic wall that was in direct contact with the grounding wire secured with the help of plastic grips.

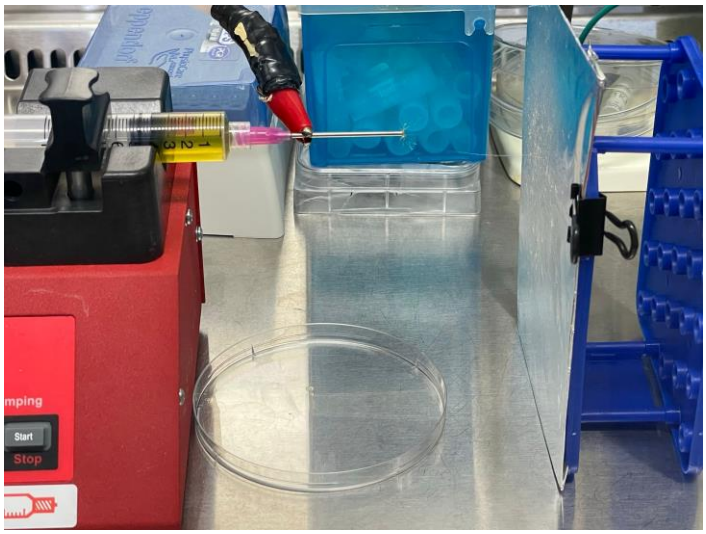

Figure 4. IMSTEL Electrospinning Apparatus. Adaption of static collector

A dynamic rotating drum collector was developed using a circular Styrofoam tube wrapped in aluminum tape mounted in a non-conductive structure. The structure was guided by a portable motor that operated on direct current (DC), withstanding enough mechanical force to rotate the collector in clockwise and counterclockwise directions. Tachometer signaling tape was located on the rotating portion to capture the rotating speed accurately.

The functioning switch was located outside the enclosure to ensure the operator's safety. Optimal rotating speed for fairly aligned fibers ranged from 100- 120 RPM.

Figure 5. IMSTEL Electrospinning Apparatus. Adaption of dynamic collector

Electrospinning of PCL based Scaffolds

PCL polymer solution with a concentration of 5.65 % w/v PCL was obtained by weighing 1.425 g of PCL and dissolving it in 25.20 mL HFP. The dissolved solution was mixed with a magnetic stirrer for 6-8 hours until a homogeneous mixture was obtained.

The polymer solution was loaded into 10 mL syringes with a 22 G (0.71 mm internal diameter) needle connected to the positive terminal of a high voltage DC supply (ES30P 10 W power supply, Gamma High Voltage Research, Ormond Beach, FL) with a voltage of 18 kV, current of 0.00-0.002 mA. The loaded syringe was placed in the syringe pump (New Era Pump Systems, Inc.). The solution was deposited at a flow rate of 0.2 mL/h during periods of 15-30 min of deposition.

The fibers were electrospun onto a grounded aluminum collector (static and dynamic) positioned 10 cm perpendicular to the needle at room temperature (70-75°F) and relative humidity of 43%.

After electrospinning, the electrospun scaffolds were rinsed with phosphate-buffered saline (pH 7.4), left to dry overnight (12h), and used for further studies. Rinsing at least a portion of the polymer solution after exposing it helps stabilize the samples. The obtained samples were stored at room temperature until further use.

Electrospinning of F-gelatin based Scaffolds

F-gelatin polymer solutions with a concentration of 5 % w/v were prepared by dissolving 0.5 g of dried F-gelatin in 10 mL of 1,1,1,3,3,3 hexafluoroisopropanol ($C_3H_2F_6O$) (HFIP). Riboflavin (RF), the visible light crosslinking photoinitiator, was obtained from ThermoFisher Scientific (Waltham, MA). This is followed by adding 100µL of RF (5% w/v in 1,1,1,3,3,3 hexafluoro-2-propanol) to the F-gelatin solution. The solution was mixed and stirred for 6–8 hours for a homogeneous blend. Prior to electrospinning, the RF solution was added to the F-gelatin solutions. The solution was stored in an aluminum-wrapped container to avoid accidental crosslinking.

The polymer solution was loaded into 10 mL syringes with a 22 G (0.71 mm internal diameter) needle connected to the positive terminal of a high voltage DC supply (ES30P 10 W power supply, Gamma High Voltage Research, Ormond Beach, FL) with a voltage of 18 kV, current of 0.02 mA. The loaded syringe was placed in the syringe pump (New Era Pump Systems, Inc.). The solution was deposited at a flow rate of 0.2 mL/h during periods of 15-30 min of deposition.

The fibers were electrospun onto a grounded aluminum collector (static and dynamic) positioned 10 cm perpendicular to the needle at room temperature (70-75°F) and relative humidity of 43%.

Following electrospinning, the resulting fibers were crosslinked by immediate exposure to visible light for 2-5 minutes (400 nm wavelengths at 100% intensity, Intelli-Ray 600, Uvitron International).

After cross-linking, the electrospun scaffolds were rinsed with phosphate-buffered saline (pH 7.4) to stabilize the samples. The samples were then stored at room temperature until further use.

Table 1. Optimized Parameters for electrospinning of F-gelatin and PCL-based fibers

Scaffold type	**F-GEL**		**PCL**	
Concentration of polymer(s)	5 % w/v		5.65 % w/v	
Solvent	1,1,1,3,3,3 HFIP			
Flow rate	0.2 mL/h			
Accelerating voltage	18 kV			
Distance tip-to-collector	10 cm			
Deposition time	30 min			
Environmental conditions (Temp – RH)	70-75 °F 43-45% RH			
Collection mode	Static	Dynamic	Static	Dynamic
Collector	Wall	Drum	Wall	Drum
Rotational Speed	N/A	100-115 RPM	N/A	100-115 RPM
Average fiber diameter	702 ±174 nm		841±357 nm	

Chapter 4: Scaffold Characterization and Validation

SCAFFOLD CHARACTERIZATION

The physiochemical characterization of the scaffolds was performed to analyze and choose an optimal scaffold as a potential platform for cardiac tissue modeling in long-term in vitro studies. The exposed polymer solution, including the biocompatible biodegradable crosslinking photoinitiator, is the basis for this analysis.

Hydrophilicity Analysis by measuring contact angle

Prior to performing degradation studies, the hydrophilicity of all samples was determined using contact angle measurement with a semi-professional camera (Canon EOS Rebel T8i EF-S 18-55mm) was used to capture a slow-motion video of a drop of water touching the surface. This procedure was repeated three times on each sample, and contact angle measurements were taken using Image J. After measurements, an average contact angle was calculated for each surface. Contact angle measurements classified surfaces as hydrophilic for angles lower than 90 degrees ($\theta < 90^{o}$) and hydrophobic for angles greater than 90 degrees ($\theta > 90^{o}$). F-gelatin coating, the contact angle on the surface is 54.38^{o}; PCL electrospun fibers have an average contact angle on the surface of 112.13^{o} degrees.

Optical Microscopy

Life Technologies (ThermoFisher) EVOS Inverted Imaging Digital Microscope was utilized to characterize electrospun scaffolds rapidly. A portion of electrospun fibers were placed on top of a glass slide and were observed at low magnifications (4X and 10X) to verify orientation and distribution.

Scanning Electron Microscopy

The majority of the analysis and micrographs were obtained through Scanning Electron Microscopy. SEM was performed to analyze the surface morphology of the electrospun scaffolds. The samples were mounted on aluminum stubs and were sputter-coated with gold for periods of 30 seconds to 2 minutes in a plasma sputter coater (JEOL Smart Coater, JEOL USA, Inc. Peabody, MA, USA) and visualized using a Hitachi SU-3500 outfitted with a backscatter electron (BSE) detector as well as an ultra-variable detector (UVD), (Hitachi America, Ltd., New York, NY, USA) at 9-10kv and current of 0.114 μA at varying magnifications, SEM (TM-1000, Hitachi, Japan) at 15kV and 33.2mA at different magnifications. Image J software was then utilized to complete analysis and data quantification.

Attenuated Total Reflection-Fourier transform infrared spectroscopy (ATR-FTIR)

ATR-FTIR was performed on electrospun scaffolds to analyze the interaction between the synthesized polymers during the electrospinning process. Measurements were performed on the fibrous scaffolds using a Thermo Mattison spectrometer (Thermo Mattison, Waltham, MA) equipped with a ZnSe ATR crystal. Typically, 32 scans were signal averaged to reduce spectral noise. The spectrum of the samples was recorded from 400 to 4000 cm^{-1} to assess the interaction between the polymers. According to the report results, the peaks match the reference's peaks at 93.72%; other databases matched between 80 - 90%. The prominent peaks between 2800 – 3000 cm^{-1} indicate the C-H functional group in CH2, and the range between 1600-1800 cm^{-1} indicates Carboxyl functional groups. These results confirm the molecular arrangement of PCL electrospun fibers.

Swelling and morphological analysis of electrospun scaffolds

Degradation studies were performed on electrospun scaffolds to assess their structural stability during long-term in vitro studies. The cross-linked electrospun scaffolds were cut in a circular pattern with a surface area of 20 mm^2 for in vitro degradation studies.

The cut specimens were placed in 12-well plates containing DMEM/F12 with 2 mM L-Glutamine, 10% FBS, and 1X Penicillin-Streptomycin Solution at 37 °C humidified with 5 % CO2 for 14 and 21 days, respectively. The specimens were recovered at the end of each degradation period and were analyzed using SEM.

MECHANICAL STABILITY OF ELECTROSPUN SCAFFOLDS

DMA Tensile Testing

A specimen of uniform cross-section is loaded in tension by a dynamic mechanical testing machine (DMA). Stress vs Strain are recorded during the test. Tensile test specimens were manufactured and sectioned following ASTM D882-18 standard for thin films. [24]. Depending on the elongation of the material and the desired properties to be gained from the testing, various speed points are utilized. Properties such as tensile stress, elongation, and modulus can be calculated. The utilized samples were prepared on the morning of the test to avoid any damage due to handling or moisture, which could represent a deterioration of the mechanical properties of the materials. [25]. DMA testing was performed using a PerkinElmer DMA 8000 (PerkinElmer, Waltham, MA, USA). The measuring system/geometry was tension-rectangle. A minimum of three specimens per sample group were tested, including three specimens for F-gelatin aligned fiber deposition, three specimens for F-gelatin random fiber deposition, three specimens for PCL aligned fiber deposition, and three for PCL random fiber deposition. The values shown in Figure 13 and Figure 14 imply a 70% representation of the actual mechanical properties of the fibers as the film itself is porous and has close to 30% spacing throughout the sample.

BIOLOGICAL ASSESSMENT OF THE ELECTROSPUN SCAFFOLDS

The biological assessment of the scaffolds was performed to analyze and choose the optimal scaffold as a potential platform for cardiac tissue modeling.

Flow cytometry analysis (FACS)

To estimate cell proliferation and overall biocompatibility of the electrospun scaffolds, the AC16 human cardiomyocytes were seeded on the electrospun scaffolds in 12-well plates (30,000 cells/well on a total area of 20mm^2) and cultured for 24 h, 3-days, and 7-days, respectively (37°C, 5% CO2).

After 24h, 3 days, and 7 days, cells on the electrospun scaffolds were treated using Trypsin-EDTA (0.25%, phenol red) to detach and extract the cells for FACS analysis.

Extracted cells were collected, stained utilizing Propidium Iodine (PI), resuspended in DMEM/F12 with 2 mM L-Glutamine, 10% FBS, and 1X Penicillin-Streptomycin Solution and added to their designated FACS analysis falcon tubes and analyzed using Beckman Coulter Gallios Flow Cytometer, (Brea, CA, USA) using excitation and emission wavelengths of 490 nm, respectively, after 24h, 3 days, and 7 days.

Positive controls included AC16 cells grown on 12-well plates with DMEM/F12 with 2 mM L-Glutamine, 10% FBS, and 1X Penicillin-Streptomycin Solution.

Negative controls included AC16 cells grown on 12-well plates treated with hydrogen peroxide 24 hours before each time point of this analysis. Hydrogen peroxide was added to all negative control wells for a final dilution of 0.1 mM.

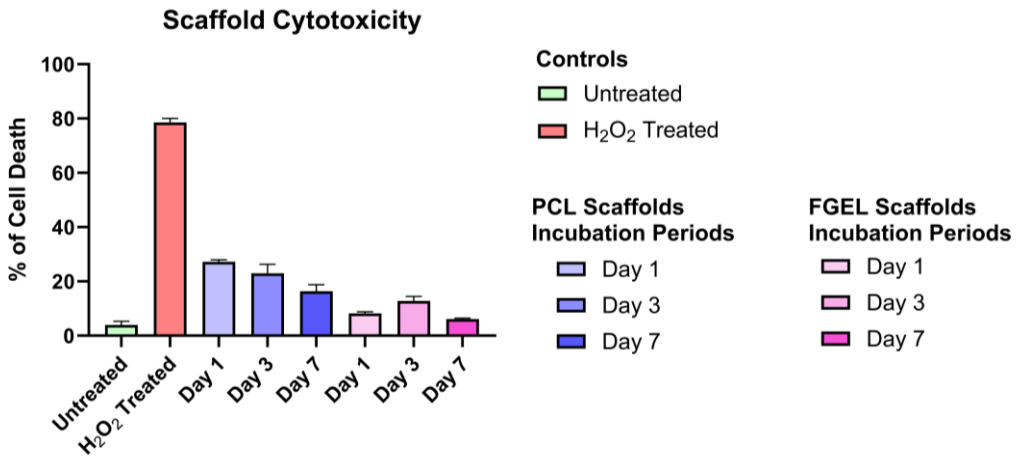

Figure 6. Scaffold cytotoxicity analysis with statistical difference of replicates

Chapter 5: Results

Fiber Orientation

Static Collector

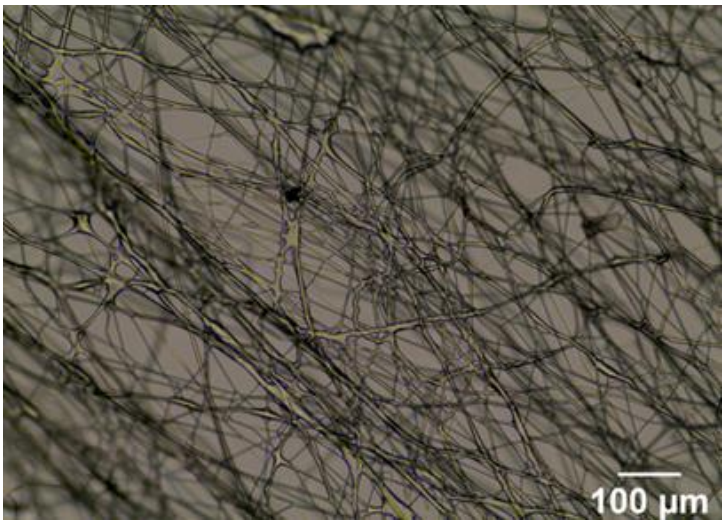

Figure 7. Random distribution of electrospun nanofibers, lacking directionality

The static collector enabled the formation of a random distribution of electrospun scaffolds, as seen in Figure 7, there is a random fiber deposition simulating a spider web formation.

Dynamic Collector

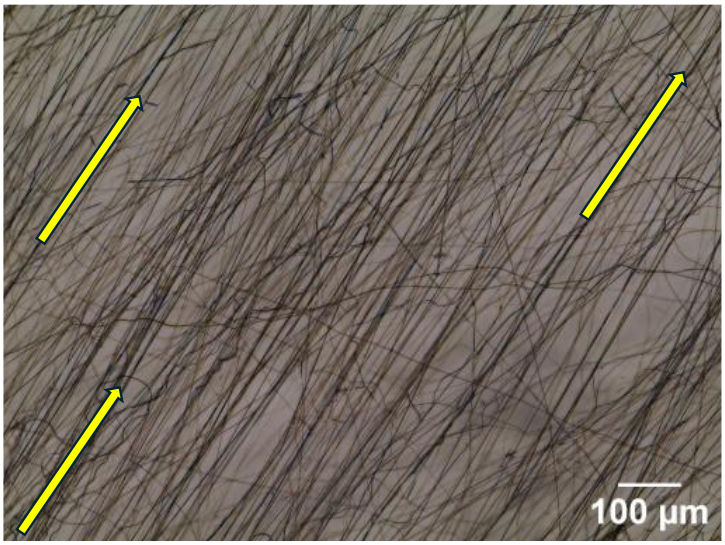

Figure 8. Fairly aligned electrospun nanofibers. Arrows depict directionality, fiber orientation

Dynamic collection enabled the formation of fairly aligned fibers.

AVERAGE FIBER SIZE

The diameters of about 100 different fiber samples were measured in each sample group using Image J to obtain their average diameter and size distribution.

Average Electrospun PCL Fiber Size

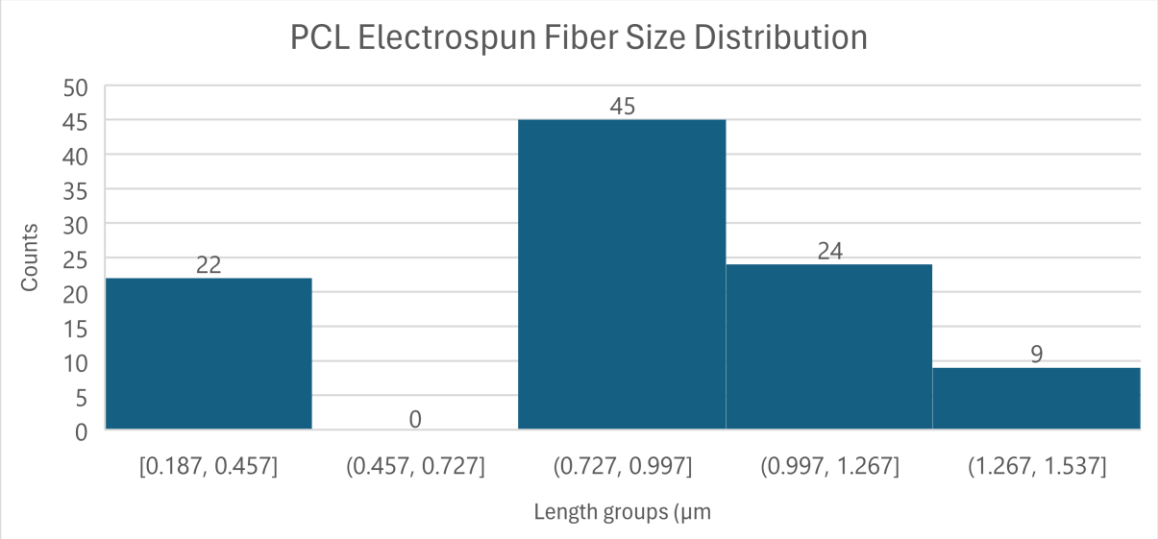

Figure 10. PCL Electrospun Fiber Size Distribution

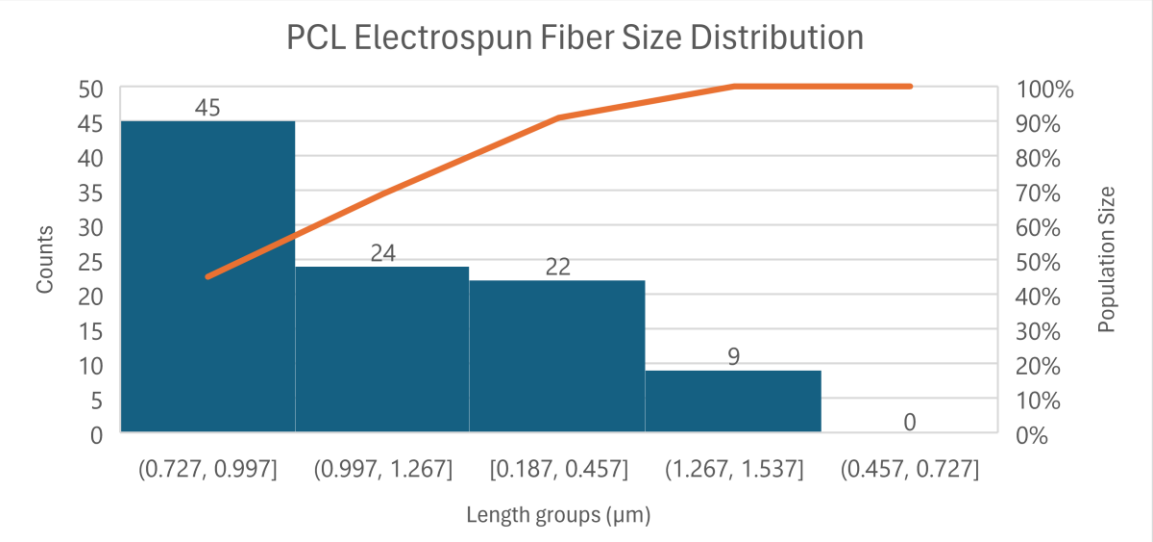

Figure 9. PCL Electrospun Fiber Size Distribution ranging from bigger to smaller size

Average Electrospun F-gelatin Fiber Size

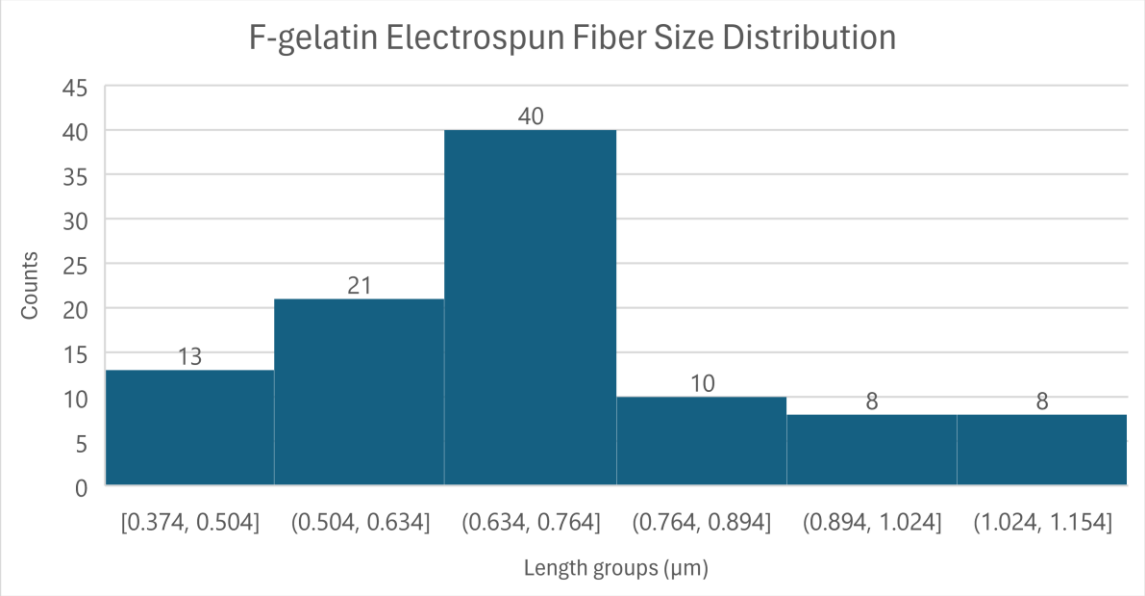

Figure 12. F-gelatin Electrospun Fiber Size Distribution

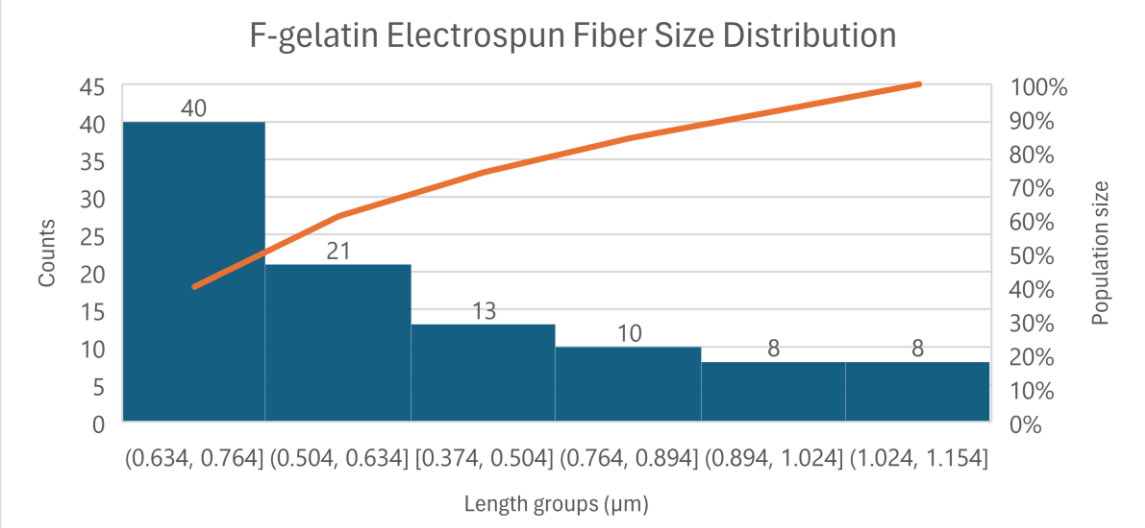

Figure 11. F-gelatin Electrospun Fiber Size Distribution ranging from bigger to smaller size

Tensile Test of Electrospun Scaffolds DMA 8000

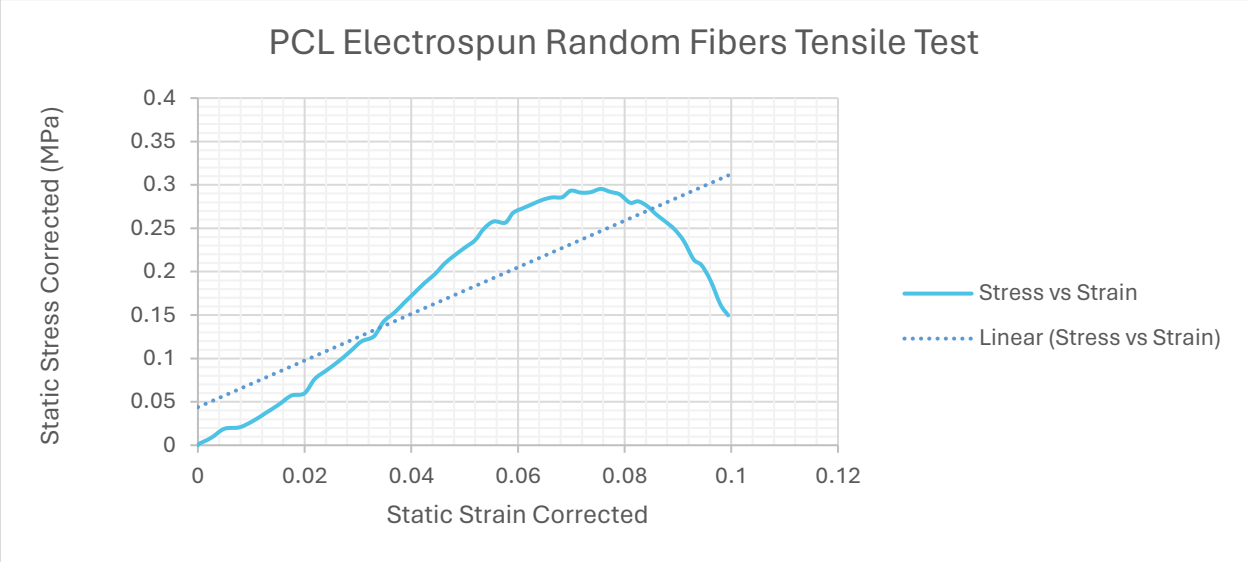

Figure 13. PCL Electrospun Fibers Tensile Test

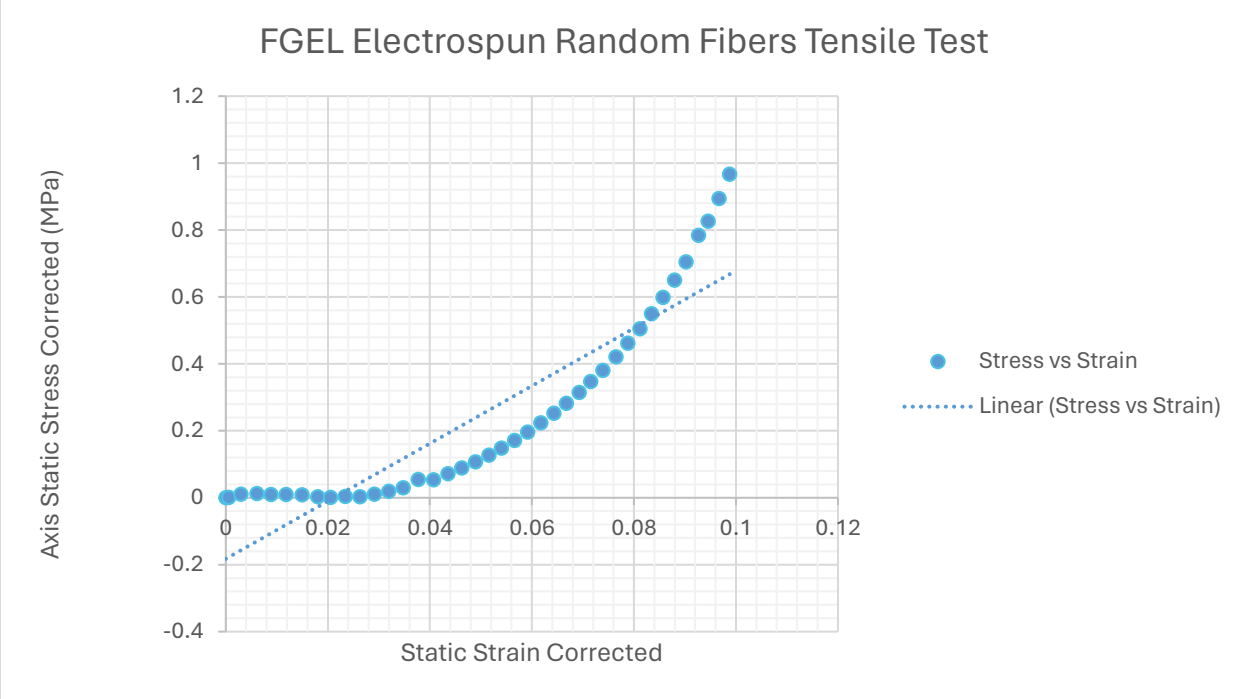

Figure 14. FGEL Electrospun Fibers Tensile Test

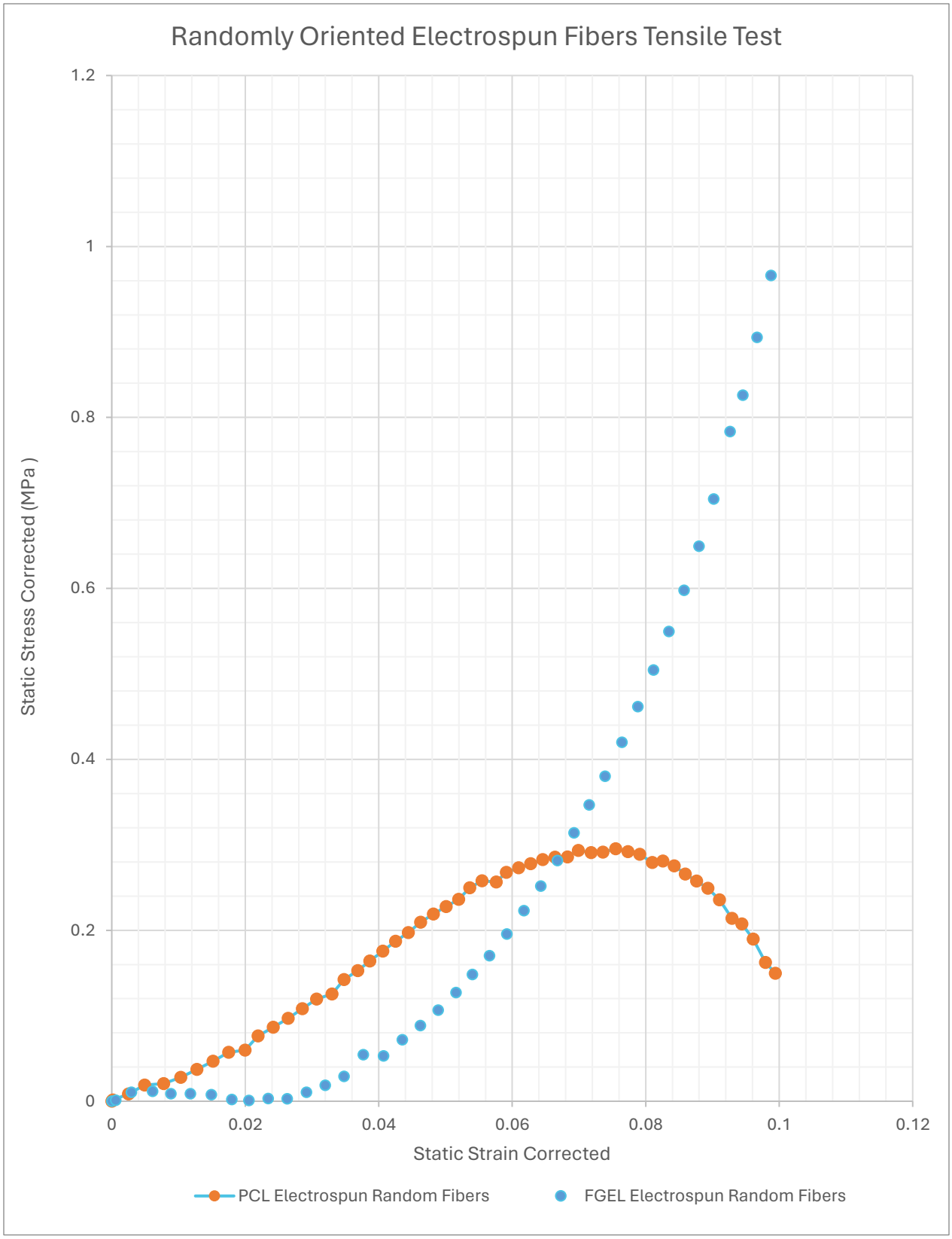

Figure 15. Random vs. Aligned PCL fibers Tensile Test, Stress vs. Strain curves

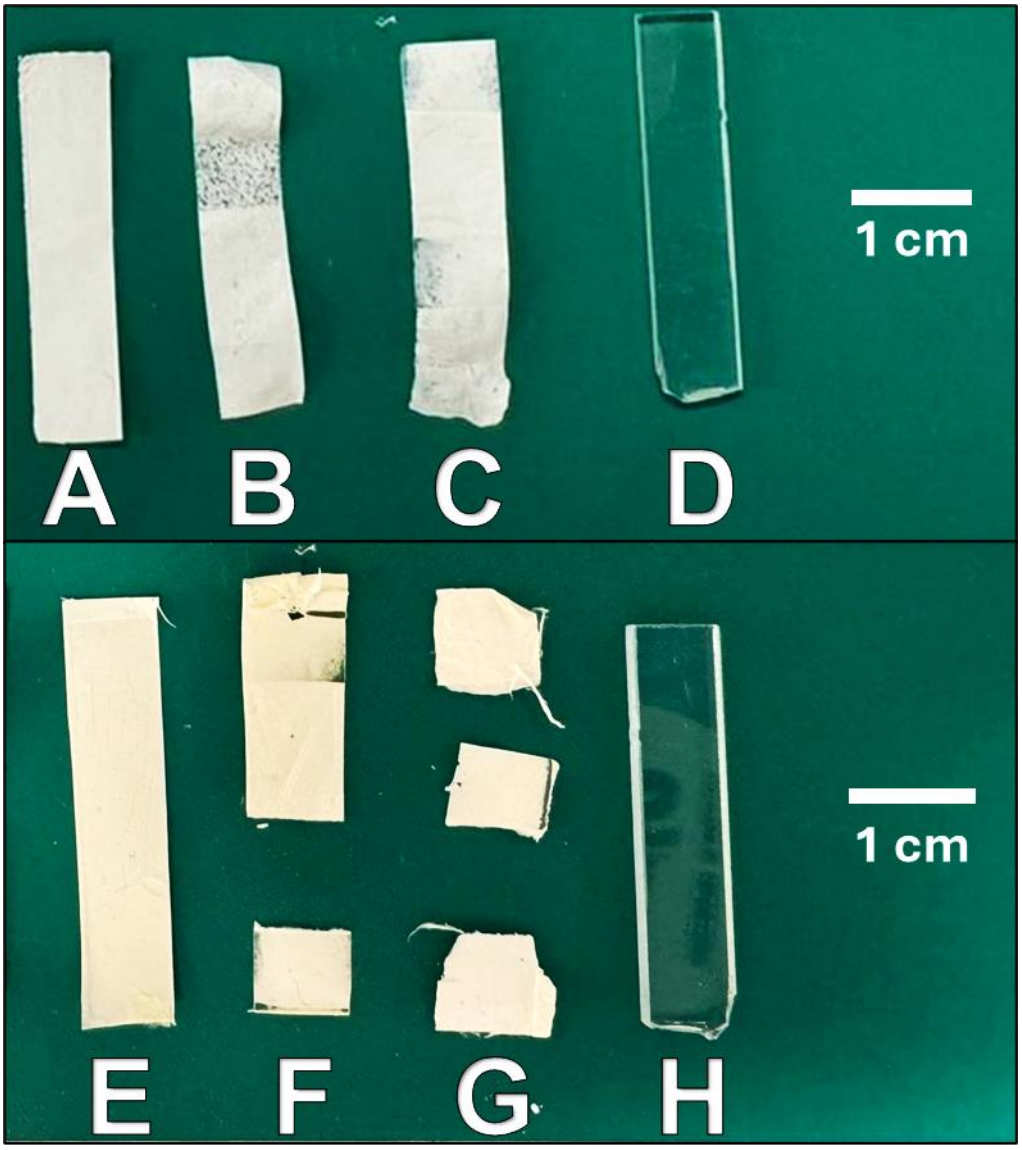

Figure 16. Macroscopy of prepared Tensile Test Specimens for Dynamic Mechanical Analyzer (DMA 8000) PCL as follows: A) Sample before testing in as-received condition, B) Aligned fibers sample after testing, C) Random fibers sample after testing, D) Control sample size. F-gelatin as follows: E) Sample before testing in as-received condition, F) Aligned fibers sample after testing, G) Random fibers sample after testing, H) Control sample size

In vitro degradation studies of electrospun scaffolds

SEM images of in vitro degradation of fibers of a PCL scaffold after 2 and 3 weeks, respectively.

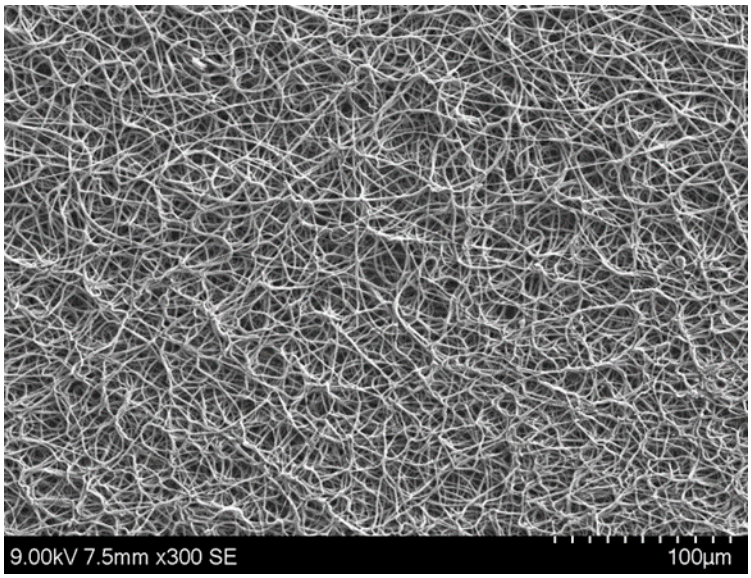

Figure 17. SEM image of in vitro degradation of fibers of a PCL scaffold after 2 weeks of exposure to PBS

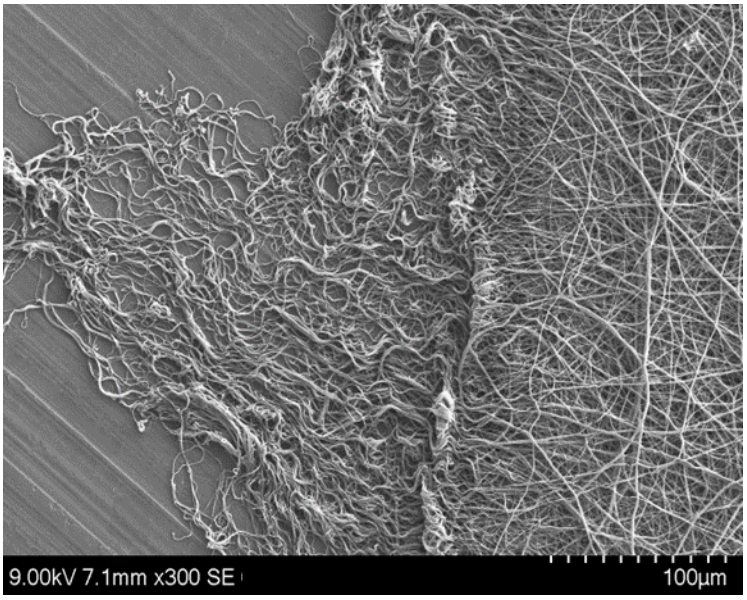

Figure 18. SEM image of in vitro degradation of fibers of a PCL scaffold after 3 weeks of exposure to PBS

SEM images of in vitro degradation of fibers of F-gelatin system immediately after exposing it to aqueous solution and after 24hrs. Swelling of the fibers was detected in all electrospun scaffolds.

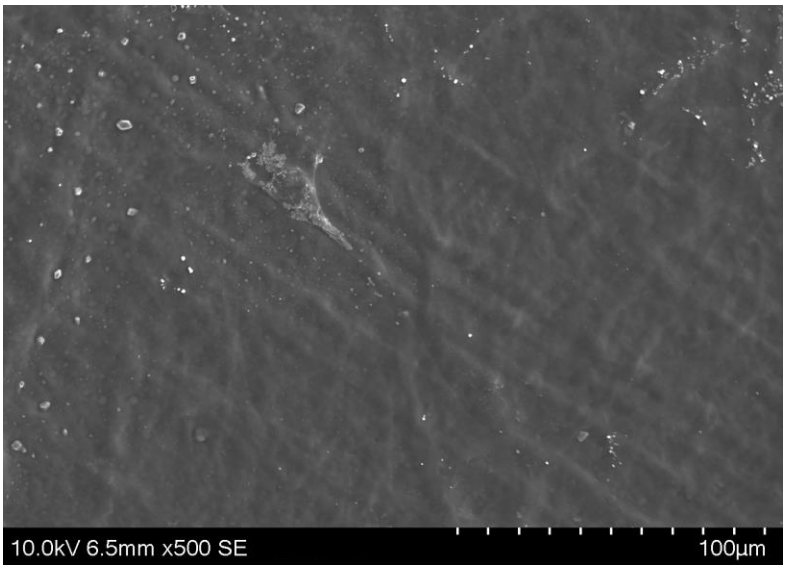

Figure 19. SEM image of in vitro degradation of fibers of F-gelatin scaffold after immediate exposure to aqueous solution

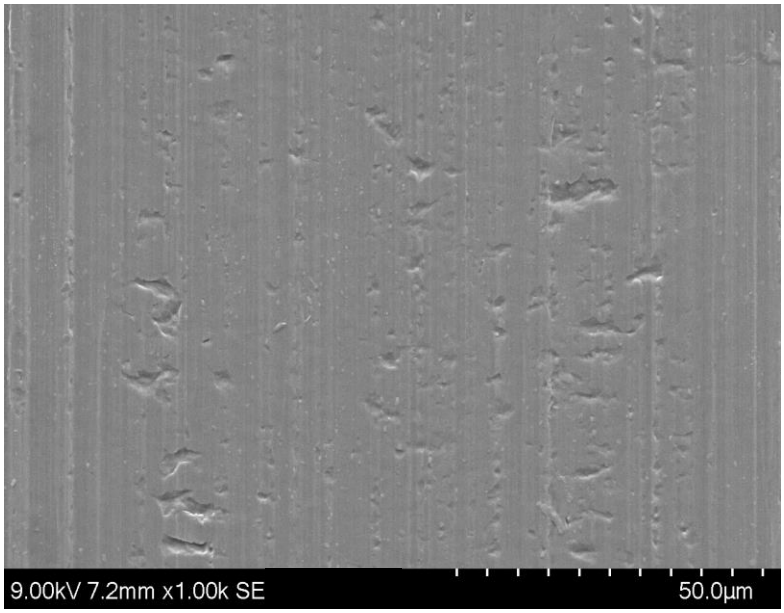

Figure 20. SEM image of in vitro degradation of fibers of F-gelatin scaffold after 24hrs. Revealing the complete dissolution of the FGEL into medium

The swelling pattern was significantly pronounced in pure F-gelatin electrospun scaffolds and least pronounced in the PCL scaffold. The degree of swelling was directly proportional to the composition of F-gelatin present in the sample. Correspondingly, changes in the morphology of the fibers were increasingly pronounced with the presence and composition of F-gelatin.

PCL, a hydrophobic polymer, was found to undergo surface erosion degradation, while gelatin in the fibers corresponded to bulk degradation of the fibers. The porosity and pore structure of the electrospun scaffolds are significantly affected by the swelling of F-gelatin.

The higher degree of swelling in F-gelatin electrospun scaffolds led to the complete occlusion of pores within 24 hours, disrupting its fibrous nature. The hydrophilicity of the gelatin structure leads to bulk degradation of the shell structure.

The results conclusively indicate that the increase in F-gelatin composition increased the biodegradability of the scaffold.

Attenuated Total Reflection-Fourier transform infrared spectroscopy (ATR-FTIR)

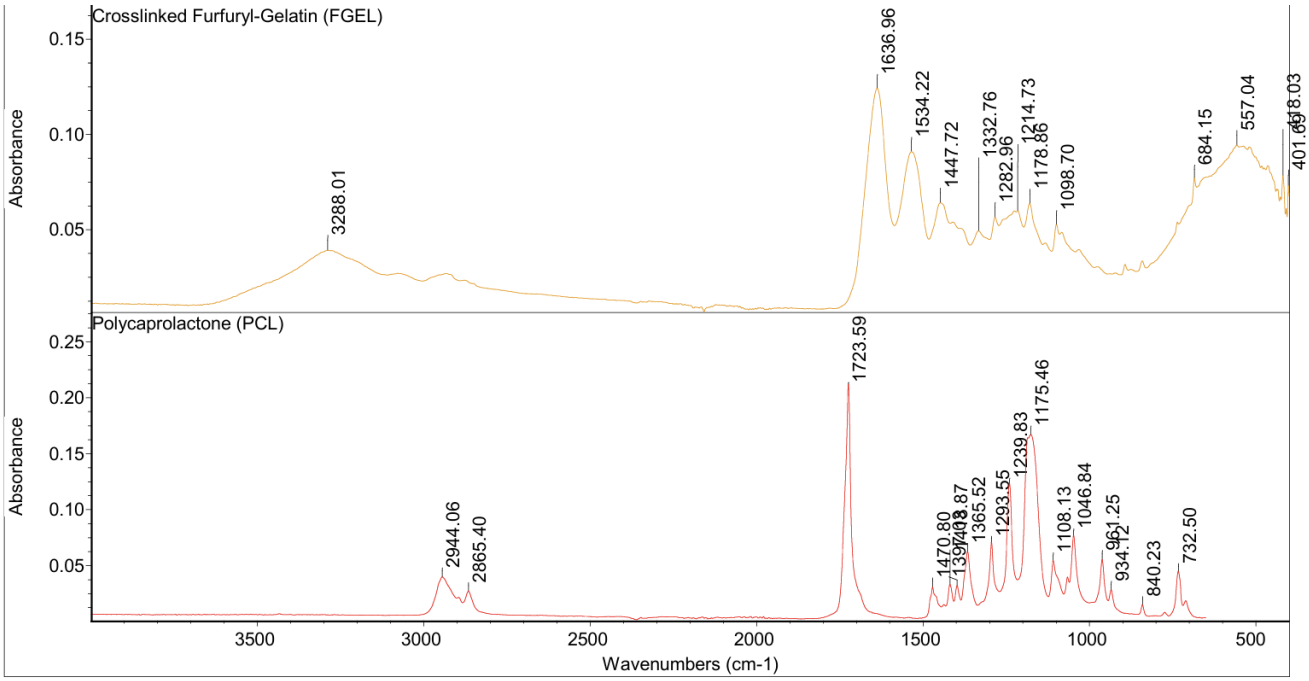

Figure 21. ATR-FTIR Analysis of Non-crosslinked F-Gelatin, and PCL

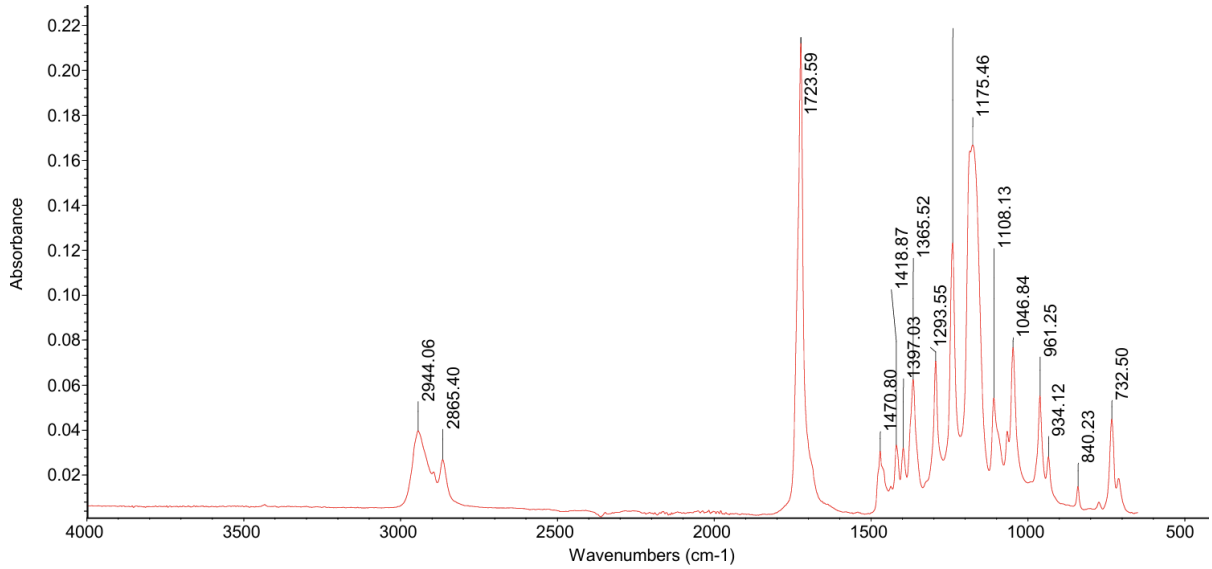

Figure 22. PCL Scaffold Fidelity Analysis via FTIR on Day1

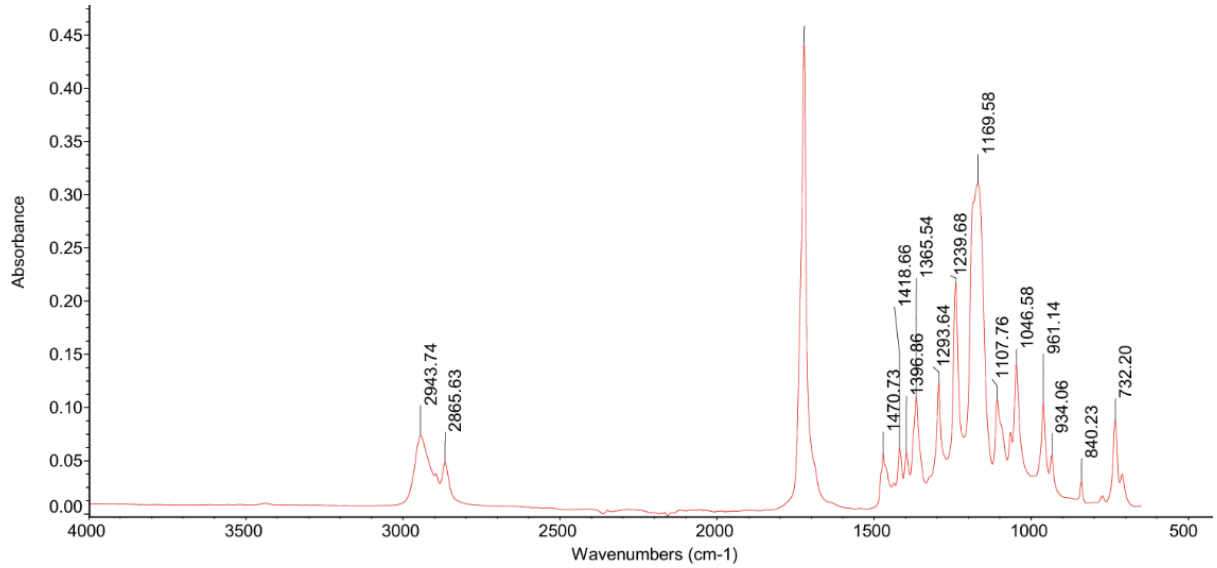

Figure 23. PCL Scaffold Fidelity Analysis via FTIR on Day 21

Flow cytometry Test - Cytotoxicity Analysis

Table 3. Optical microscopy of 2D cell culture of AC16 cardiomyocytes.
Positive and Negative control groups for cytotoxicity at different time points, day 1, day 3, and day 7

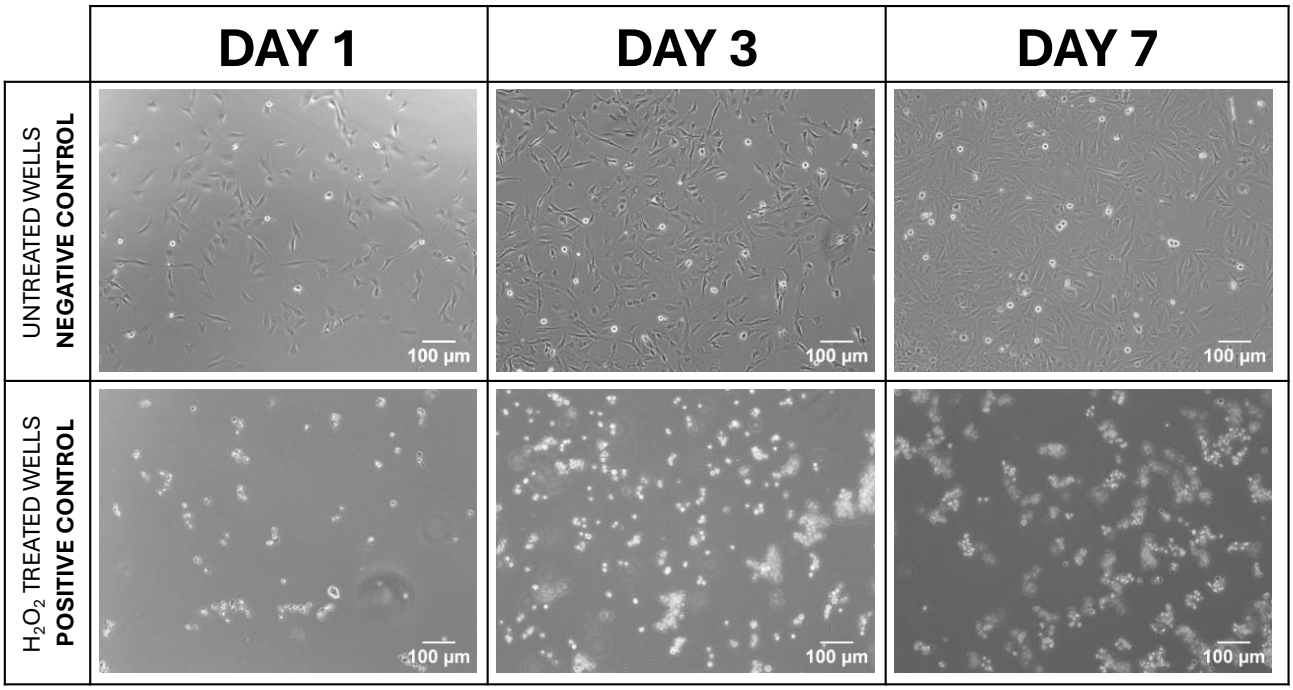

Table 2. Cytotoxicity Study via flow cytometry PCL vs F-gelatin on day 1, day 3, and day 7.
"L" depicts the percentage of live cells, and "D" represents the percentage of dead cells

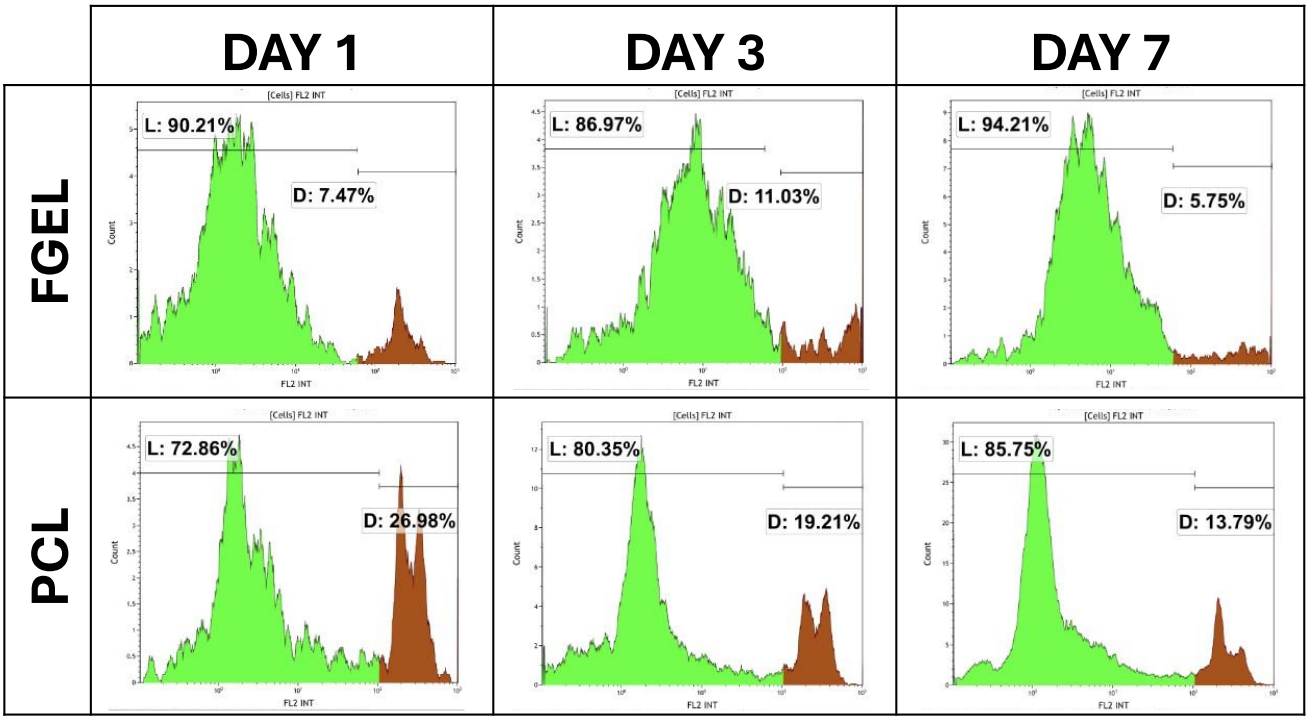

Table 4. Cytotoxicity Study via flow cytometry. Positive and Negative Controls on Day 7. "L" depicts the percentage of live cells, and "D" represents the percentage of dead cells

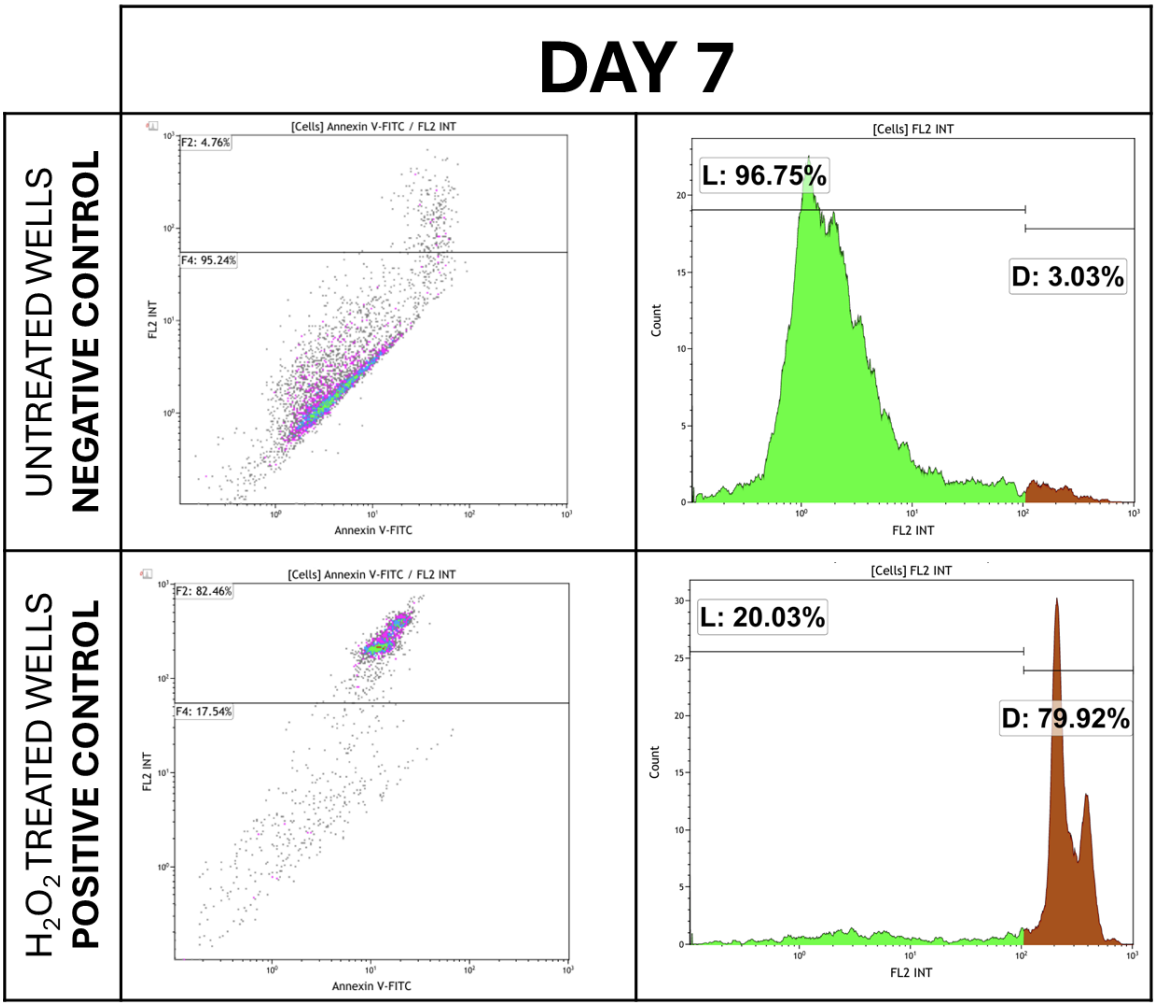

Chapter 6: Conclusion

Critical Analysis and Conclusions

The development of nanofiber-composed film provides a matrix with comparable properties to native tissue, allowing further study applications in the tissue engineering field.

The proposed method showed that as the collector rotations per minute increase, so does the alignment of the deposited fibers.

3D scaffold matrix provided a greater seeding area for cell culture, which, after long viability studies, showed improved proliferation and cell interaction.

The results conclusively indicate that the increase in F-gelatin composition increased the biodegradability of the scaffold.

Broader Impacts and Future Directions

The cellular compatibility of the aligned electrospun film will be evaluated for cardiac and neuronal applications by seeding and differentiation of neural progenitor cells for studying neurodegenerative diseases.

Further studies include the development of aligned coaxial electrospun fibers of the polycaprolactone and furfuryl gelatin to develop cardiac cell models to study the onset of diabetes and myocardial infractions.

Analysis of cell viability of aligned electrospun scaffolds of the polycaprolactone and furfuryl gelatin to develop cardiac cell models adopting the tissue-on-a-chip models.

Analysis of Matrigel coatings for electrospun scaffolds adopting the tissue-on-a-chip models to be tested under microgravity and other extreme environmental conditions will be performed.

Further studies will evaluate an A-B-A-B multilayer system that will look to incorporate two or more different scaffolds in order to build an integrated system that possesses diverse properties and thus expands its applications in the tissue engineering field.

References

[1] Mazaki, T., Shiozaki, Y., Yamane, K.et al. A novel, visible light-induced, rapidly cross-linkable gelatin scaffold for osteochondral tissue engineering. SciRep 4,4457 (2014).

[2] Son TI, et al. Visible light-induced crosslinkable gelatin. ActaBiomaterialia.2010; 6(10):4005–4010

[3] Kumar, S.A et al. The applicability of furfuryl-gelatin as a novel bioink for tissue engineering applications. J Biomed. Mat. Res. B 2019;107(2):314-323.

[4] Nagiah, Naveen, et al. "Stem Cell− Laden Coaxially Electrospun Fibrous Scaffold for Regenerative Engineering Applications." Current Protocols1.1 (2021): e13.5. Raheja, A., et al. Design of low-cost spinneret assembly for coaxial electrospinning. Appl. Phys. Lett.106, 254101 (2015)

[5] Son, T. il, Sakuragi, M., Takahashi, S., Obuse, S., Kang, J., Fujishiro, M., Matsushita, H., Gong, J., Shimizu, S., Tajima, Y., Yoshida, Y., Suzuki, K., Yamamoto, T., Nakamura, M., & Ito, Y. (2010). Visible light-induced crosslinkable gelatin. Acta Biomaterialia, 6(10). https://doi.org/10.1016/j.actbio.2010.05.018

[6] Rahmati, M., Mills, D. K., Urbanska, A. M., Saeb, M. R., Venugopal, J. R., Ramakrishna, S., & Mozafari, M. (2021). Electrospinning for tissue engineering applications. In Progress in Materials Science (Vol. 117). https://doi.org/10.1016/j.pmatsci.2020.100721

[7] Kalantari, K., Afifi, A. M., Jahangirian, H., & Webster, T. J. (2019). Biomedical applications of chitosan electrospun nanofibers as a green polymer – Review. In Carbohydrate Polymers (Vol. 207). https://doi.org/10.1016/j.carbpol.2018.12.011

[8] Bhardwaj, N., & Kundu, S. C. (2010). Electrospinning: A fascinating fiber fabrication technique. In Biotechnology Advances (Vol. 28, Issue 3). https://doi.org/10.1016/j.biotechadv.2010.01.004

[9] Tonda-Turo, C., Ruini, F., Ramella, M., Boccafoschi, F., Gentile, P., Gioffredi, E., Falvo D'Urso Labate, G., & Ciardelli, G. (2017). Non-covalently crosslinked chitosan nanofibrous mats prepared by electrospinning as substrates for soft tissue regeneration. Carbohydrate Polymers, 162. https://doi.org/10.1016/j.carbpol.2017.01.050

[10] Tokiwa, Y., & Suzuki, T. (1977). Hydrolysis of polyesters by lipases. *Nature*, *270*(5632). https://doi.org/10.1038/270076a0

[11] Nair, N. R., Sekhar, V. C., Nampoothiri, K. M., & Pandey, A. (2016). Biodegradation of Biopolymers. In Current Developments in Biotechnology and Bioengineering: Production, Isolation and Purification of Industrial Products. https://doi.org/10.1016/B978-0-444-63662-1.00032-4

[12] Malikmammadov, E., Tanir, T. E., Kiziltay, A., Hasirci, V., & Hasirci, N. (2018). PCL and PCL-based materials in biomedical applications. Journal of Biomaterials Science, Polymer Edition, 29(7–9). https://doi.org/10.1080/09205063.2017.1394711

[13] AnilKumar, S., Allen, S. C., Tasnim, N., Akter, T., Park, S., Kumar, A., Chattopadhyay, M., Ito, Y., Suggs, L. J., & Joddar, B. (2019). The applicability of furfuryl-gelatin as a novel bioink for tissue engineering applications. Journal of Biomedical Materials Research - Part B Applied Biomaterials, 107(2). https://doi.org/10.1002/jbm.b.34123

[14] Nagiah, N., el Khoury, R., Othman, M. H., Akimoto, J., Ito, Y., Roberson, D. A., & Joddar, B. (2022). Development and Characterization of Furfuryl-Gelatin Electrospun Scaffolds for Cardiac Tissue Engineering. ACS Omega, 7(16). https://doi.org/10.1021/acsomega.2c00271

[15] Park, S. H., Seo, S. Y., Kang, J. H., Ito, Y., & Son, T. il. (2013). Preparation of photocured azidophenyl-fish gelatin and its capturing of human epidermal growth factor on titanium plate. Journal of Applied Polymer Science, 127(1). https://doi.org/10.1002/app.37854

[16] Mazaki, T., Shiozaki, Y., Yamane, K., Yoshida, A., Nakamura, M., Yoshida, Y., Zhou, D., Kitajima, T., Tanaka, M., Ito, Y., Ozaki, T., & Matsukawa, A. (2014). A novel, visible light-induced, rapidly cross-linkable gelatin scaffold for osteochondral tissue engineering. Scientific Reports, 4. https://doi.org/10.1038/srep04457

[17] *Adel, M., Keyhanvar, P., Zare, I., Tavangari, Z., Akbarzadeh, A., & Zahmatkeshan, M. (2023). Nanodiamonds for tissue engineering and regeneration. Journal of Drug Delivery Science and Technology, 90. https://doi.org/10.1016/j.jddst.2023.105130

[18] Zhong, W. (2016). Nanofibres for medical textiles. In Advances in Smart Medical Textiles (pp. 57-70). Woodhead Publishing.

[19] Zhao, K., Kang, S. X., Yang, Y. Y., & Yu, D. G. (2021). Electrospun functional nanofiber membrane for antibiotic removal in water. Polymers, 13(2), 226.

[20] Akdere, M., & Schneiders, T. (2021). Modeling of the electrospinning process. In Advances in Modeling and Simulation in Textile Engineering (pp. 237-253). Woodhead Publishing.

[21] Thomas, S., Kalarikkal, N., Oluwafemi, O. S., & Wu, J. (Eds.). (2019). Nanomaterials for Solar Cell Applications. Elsevier. https://makeagif.com/gif/electrospinning-of-pvoh-nanofibres-captured-at-7276-fps-xK8ju_

[22] Bridge, J. C., Aylott, J. W., Brightling, C. E., Ghaemmaghami, A. M., Knox, A. J., Lewis, M. P., Rose, F. R. A. J., & Morris, G. E. (2015). Adapting the electrospinning process to provide three unique environments for a tri-layered in vitro model of the airway wall. Journal of Visualized Experiments, (101). https://doi.org/10.3791/52986

[23] Türker, E., Yildiz, Ü. H., & Arslan Yildiz, A. (2019). Biomimetic hybrid scaffold consisting of co-electrospun collagen and PLLCL for 3D cell culture. International Journal of Biological Macromolecules, 139. https://doi.org/10.1016/j.ijbiomac.2019.08.082

[24] ASTM (2018) ASTM D882-18: Standard test method for tensile properties of thin plastic films. ASTM

[25] Quiñonez, P. A., Ugarte-Sanchez, L., Bermudez, D., Chinolla, P., Dueck, R., Cavender-Word, T. J., & Roberson, D. A. (2021). Design of shape memory thermoplastic material systems for fdm-type additive manufacturing. Materials, 14(15). https://doi.org/10.3390/ma14154254

Vita

Zayra Naomi Dorado, Metallurgical and Materials Engineer, graduated from the University of Texas at El Paso (UTEP) with a concentration in Biomedical Engineering. She graduated in the Fall of 2021 and was awarded the Henry P. Ehrlinger as an Outstanding Graduate in Metallurgical Engineering. She was awarded the Pathways to Success in Graduate Engineering (PASSE) scholarship. As an NSF Graduate Scholar, she continued her studies in graduate school in Metallurgical and Materials Engineering with a professional certification in Additive Manufacturing and 3D Technologies.

She has worked as a Graduate Research Assistant under Dr. Joddar's mentorship at IMSTEL. Her relevant work experience includes working in diverse areas, including new technology implementation, forensic failure analysis, quality control and assurance, and several research investigations related to the development of new biomedical devices, water testing and control of contaminants, evaluation of corrosion in structures, and identification of failure causes in tested pieces, providing recommendations for material selection. Zayra has experience implementing new projects in several industries, including biomedical, automobile, water treatment, and aerospace.

This work has been filed in part under patent US18302553 and submitted for publication. Zayra plans to continue her career in engineering to make further contributions in the field.

Contact Information: zayranaomi@gmail.com